Section 6

Developments in global forecast models, case studies, predictability investigations, global ensembles.

Hindcast verification of JMA's GEPS for one-month prediction

SEKIGUCHI Ryohei, ICHIKAWA Yuiko, OCHI Kenta, and TAKAKURA Toshinari
Japan Meteorological Agency
(E-mail: t-takakura@met.kishou.go.jp)

1. Introduction

The Japan Meteorological Agency (JMA) upgraded its Global Ensemble Prediction System (GEPS) in March 2022 to incorporate recent Global Spectral Model (GSM) developments, horizontal resolution enhancement, improvement of sea surface temperature (SST) boundary conditions and tuning of initial perturbation amplitude (Yamaguchi et al. 2022). This paper outlines GEPS performance in one-month prediction based on 30-year hindcast experiments.

2. Hindcast Experiments

Experiments were conducted for 1991 to 2020 for the new GEPS ("TEST" in Table 1) and the previous GEPS version ("CNTL1"), with the latest Japanese reanalysis (JRA-3Q; Kobayashi et al. 2021) for atmospheric initial conditions. Initial perturbations were created from a combination of initial singular vectors (SVs) and evolved SVs, differently from the operational system approach (Sekiguchi et al. 2018).

In previous hindcast experiments, the Japanese 55-year Reanalysis (JRA-55; Kobayashi et al. 2015) was used for atmospheric initial conditions. To evaluate the effects of atmospheric initial condition updating, additional experimentation was conducted with the previous version of GEPS using the JRA-55 as atmospheric initial conditions ("CNTL2" in Table 1).

3. Verification

The results indicated that forecasting with the new GEPS was superior to that of the previous GEPS for several elements and seasons, especially in the tropics. Figure 1 shows improved anomaly correlation coefficients (ACCs) for surface temperature in the Northern Hemisphere and velocity potential at 200 hPa in the tropics. The ACCs of the new GEPS were also compared with those of the previous GEPS using JRA-55 as atmospheric initial conditions. As per Figure 2, forecast skill was further improved due to the upgraded atmospheric initial conditions. The characteristics of forecast mean errors for the new GEPS were generally comparable to those of the previous GEPS (not shown).

Prediction skill for Madden-Julian oscillation (MJO) was evaluated using the method described by Matsueda and Takaya (2012). As per Figure 3, MJO forecast skill was improved in forecasts with lead times of 10 days or more. The biases of predicted MJO amplitude and the phase speed of the new GEPS were generally comparable to those of the previous GEPS (not shown).

References

Hersbach, H., B. Bell, P. Berrisford, S. Hirahara, A Hornyi, J. Muoz-Sabater, J. Nicolas, C. Peubey, R. Radu, D. Schepers, A. Simmons, C. Soci, S. Abdalla, X. Abellan, G. Balsamo, P. Bechtold, G. Biavati, J. Bidlot, M. Bonavita, G. De Chiara, P. Dahlgren, D. Dee, M. Diamantakis, R. Dragani, J. Flemming, R. Forbes, M. Fuentes, A. Geer, L. Haimberger, S. Healy, R. J. Hogan, E. Hlm, M. Janiskov, S. Keeley, P. Laloyaux, P. Lopez, C. Lupu, G. Radnoti, de P. Rosnay, I. Rozum, F. Vamborg, S. Villaume, and J.-N. Thpaut, 2020: The ERA5 global reanalysis. *Quart. J. Roy. Meteor. Soc.*, 146, 1999{2049, doi:10.1002/qj.38 03.

Kobayashi, S., Y. Ota, Y. Harada, A. Ebita, M. Moriya, H. Onoda, K. Onogi, H. Kamahori, C. Kobayashi, H. Endo, K. Miyaoka, and K. Takahashi, 2015: The JRA-55 reanalysis: General specifications and basic characteristics. *J. Meteor. Soc. Japan.*, **93**, 5-48.

Kobayashi, S., Y. Kosaka, J. Chiba, T. Tokuhiro, Y. Harada, C. Kobayashi, and H. Naoe, 2021: JRA-3Q: Japanese reanalysis for three quarters of a century. *WCRP-WWRP Symposium on Data Assimilation and Reanalysis/ECMWF annual seminar 2021*, WMO/WCRP, O4-2, https://symp-bonn2021.sciencesconf.org/data/355900.pdf.

Matsueda, S., and Y. Takaya, 2012: Forecast skill of MJO with the JMA's One-month Ensemble Prediction System. *CAS/JSC WGNE Res. Activ. Atmos. Oceanic Modell.*, **42**, 6.11-6.12.

Sekiguchi, R., Y. Adachi, T. Kanehama, Y. Kubo, K. Miyaoka, A. Nishimura, A. Shimpo, and T. Yoshida, 2018: Verification of JMA's new GEPS for one-month prediction. *WGNE. Res. Activ. Earth Sys. Modell.*, **48**, 6.11-6.12.

Takakura, T., and T. Komori, 2020: Two-tiered sea surface temperature approach implemented to JMA's Global Ensemble Prediction System. *WGNE. Res. Activ. Earth Sys. Modell.*, **50**, 6.15-6.16.

Ujiie, M., M. Higuchi, T. Kadowaki, Y. Kuroki, K. Miyaoka, M. Oda, K. Ochi, R. Sekiguchi, H. Shimizu, S. Yokota, and H. Yonehara, 2021: Upgrade of JMA's Operational Global NWP system. *WGNE. Res. Activ. Earth Sys. Modell.*, **51**, 6.09-6.10.

Yamaguchi, H., Y. Adachi, S. Hirahara, Y. Ichikawa, T. Iwahira, Y. Kuroki, C. Matsukawa, R. Nagasawa, K. Ochi, R. Sekiguchi, T. Takakura, M. Ujiie, and H. Yonehara, 2022: Upgrade of JMA's Global Ensemble Prediction System. *WGNE Res. Activ. Earth Sys. Modell.*, submitted.

Table 1 Hindcast experiments

	TEST	CNTL1	CNTL2
Atmospheric forecast model	GSM2103 with improved physical processes (Yamaguchi et al. 2022)	GSM2103 (Ujiie et al. 2021)	
Resolution (model top)	TQ479L128 (0.01 hPa) up to 18 days TQ319L128 (0.01 hPa) afterward	TL479L128 (0.01 hPa) up to 18 days TL319L128 (0.01 hPa) afterward	
Initial conditions (atmosphere)	JRA-3Q (Kobayashi et al. 2021)		JRA-55 (Kobayashi et al. 2015)
Initial conditions (land)	Offline runs of land-surface model in GEPS and atmospheric forcing from JRA-3Q		Offline runs of land-surface model in GEPS and atmospheric forcing from JRA-55
Sea surface temperature (SST)	Two-tiered SST approach (Takakura and Komori 2020) with improvement	Two-tiered SST approach	
Initial perturbation	Singular vector (SV) method (initial and evolved SVs)		
Period (initial date)	1991 – 2020 (15th and end of calendar month)		
Ensemble size	13		
Verification data	JRA-3Q, ERA5 (Hersbach et al. 2020)		

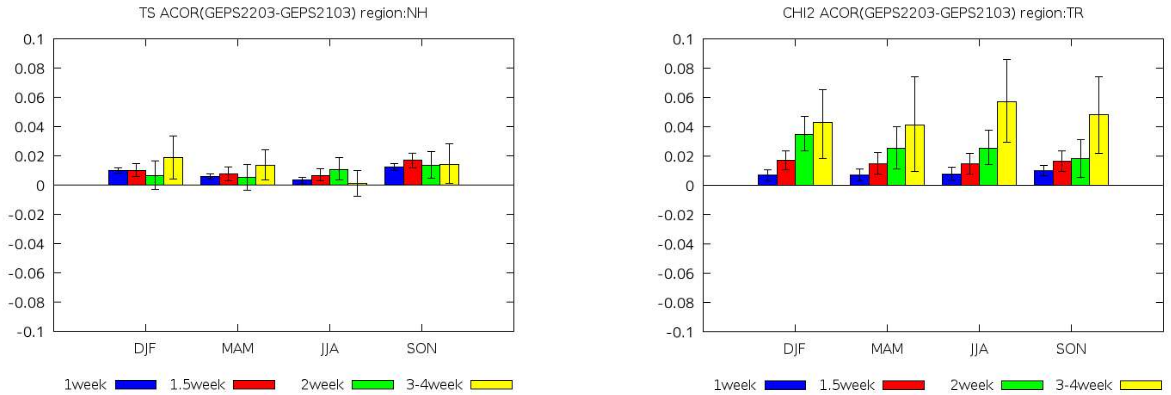

Figure 1 Anomaly correlation coefficient (ACC) differences of TEST from CNTL1 for (left) surface temperature in the Northern Hemisphere (20－90°N) and (right) velocity potential at 200 hPa in the Tropics (20°S－20°N) for all seasons. Positive values represent ACCs of TEST exceeding those of CNTL1. Error bars indicate two-sided 95% confidence levels. ACCs are calculated against JRA-3Q.

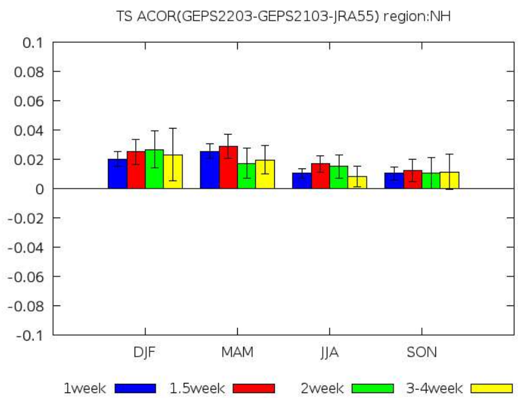

Figure 2 ACC differences of TEST from CNTL2 for surface temperature in the Northern Hemisphere for all seasons
Positive values represent ACCs of TEST exceeding those of CNTL2. ACCs are calculated against ERA5.

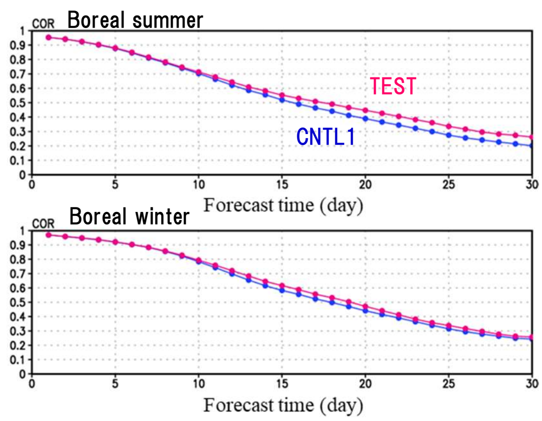

Figure 3 Correlation coefficients of the MJO index for (top) boreal summer and (bottom) boreal winter
Red and blue lines represent results for TEST and CNTL1, respectively.

Assessing the feasibility for Atmosphere-Ocean Coupling of JMA's Global Ensemble Prediction System

TAKAKURA Toshinari[1,*], OCHI Kenta[1], ADACHI Yukimasa[2] and KOMORI Takuya[1]
1: Numerical Prediction Division, Japan Meteorological Agency
2: Meteorological Research Institute, Japan Meteorological Agency
E-mail: t-takakura@met.kishou.go.jp

1. Introduction

The Global Ensemble Prediction System (GEPS) operated by the Japan Meteorological Agency (JMA) incorporates an atmospheric model with a two-tiered sea surface temperature (SST) approach (Takakura and Komori 2020) for lower boundary conditions. This technique indirectly represents atmosphere-ocean interaction by combining SSTs prescribed as persisting anomalies from climatological SSTs and SSTs operationally precomputed using JMA's seasonal EPS. In the work reported here, feasibility for atmosphere-ocean coupling of GEPS was assessed toward the incorporation of more directly representative atmosphere-ocean interaction.

2. Experimental design

(1) Retrospective forecast experiments

Retrospective forecast experiments covering winter 2019/20 and summer 2020 were conducted with focus on initial shocks caused by inconsistencies between the lower boundary specifications of the atmospheric model in coupling prediction and atmospheric analysis representing initial conditions. Only a control member was run, and the forecast time was limited to 264 hours. The first experiment (CNTL) was conducted using the currently operational GEPS (Yamaguchi et al. 2022). In the next experiment (CPL), atmosphere-ocean coupling was applied to CNTL using an ocean model with specifications similar to those of the seasonal EPS (JMA/MRI-CPS3; Kubo and Ochi 2022). In the last experiment (CPL2), mixed land-ocean-lake grid and sea-ice coupling were switched off to reduce the initial shocks seen in CPL. Furthermore, tendency coupling (e.g., Mogensen et al. 2017) was applied to SSTs at mid- and high latitudes in CPL2 up to 132 hours and linear relaxation to full coupling was applied from 132 to 264 hours by adding the tendency of the SST in the ocean model to SST analysis values.

(2) 30-year (1991 – 2020) hindcast experiments

Hindcast experiments for CNTL, CPL and CPL2 were conducted with the same specifications as Sekiguchi et al. (2022), except for an ensemble size of 5, a forecast time up to 438 hours and initial dates of three days for each of summer and winter.

3. Results

Figure 1 shows the initial shocks of CPL and CPL2 against CNTL in the root mean square error (RMSE) differences of zonal mean temperature with lead times of 24 hours in the retrospective forecast experiments. The larger RMSE in the lower atmosphere of CPL presumably resulted from differences in SST, sea-ice and mixed land-ocean-lake grid specifications between coupling prediction and atmospheric analysis. CPL2 exhibited reduced deterioration in RMSE at high latitudes via the switching off of the mixed land-ocean-lake grid and sea-ice coupling and at mid-latitudes due to tendency coupling effects.

To evaluate the impact of tendency coupling, anomaly correlation coefficients (ACCs) of SSTs were compared over week 1 of the hindcast experiment (Figure 2). ACCs in CPL were better in the tropics and the summer hemisphere than those of CNTL, but worse in mid-latitude eddy-rich oceanic regions. The deterioration in these regions is attributed to inadequate representation of meso-scale ocean eddies in the ocean model with 0.25-degree resolution. Meanwhile, CPL2 exhibited reduced deterioration in the mid-latitudes because the high spatial variability of SST analysis is maintained in tendency coupling. As a result, the bias-corrected ACCs of CPL2 were superior to those of CNTL for many atmospheric scores in the hindcast experiments (Figure 3). ACC without bias correction also shows better scores except for 850 hPa temperatures in the Tropics, where there is an influence from the cold SST bias of the coupled model (not shown). Overall, including the improved Madden-Julian Oscillation (MJO) forecast skill contributed by better atmospheric circulation (Figure 4), the CPL2 results are promising for further GEPS development.

References

Kobayashi, S., Y. Kosaka, J. Chiba, T. Tokuhiro, Y. Harada, C. Kobayashi, and H. Naoe, 2021: JRA-3Q: Japanese reanalysis for three quarters of a century. *WCRP-WWRP Symposium on Data Assimilation and Reanalysis/ECMWF annual seminar 2021*, WMO/WCRP, O4-2, https://symp-bonn2021.sciencesconf.org/data/355900.pdf.

Kubo Y., and K. Ochi, 2022: Verification of JMA/MRI-CPS3 and JMA Global Ensemble Prediction System in the sub-seasonal forecast. *WGNE Res. Activ. Earth Sys. Modell*., submitted.

Matsueda, M., and H. Endo, 2011: Verification of medium-range MJO forecasts with TIGGE. *Geophys. Res. Lett*., **38**, L11801.

Merchant, C.J., Embury, O., Roberts-Jones, J., Fiedler, E., Bulgin, C.E., Corlett, G.K., Good, S., McLaren, A., Rayner, N., Morak-Bozzo, S. and Donlon, C. (2014), Sea surface temperature datasets for climate applications from Phase 1 of the European Space Agency Climate Change Initiative (SST CCI). *Geosci. Data J*., **1**, 179-191.

Mogensen, K.S., L. Magnusson and J-R. Bidlot, 2017: Tropical Cyclone Sensitivity to Ocean Coupling *ECMWF Technical Memorandum*, **794**.

Sekiguchi, R., Y. Ichikawa, K. Ochi, and T. Takakura, 2022: Hindcast verification of JMA's GEPS for one-month prediction. *WGNE Res. Activ. Earth Sys. Modell*., submitted.

Takakura, T., and T. Komori, 2020: Two-tiered sea surface temperature approach implemented to JMA's Global Ensemble Prediction System. *WGNE. Res. Activ. Earth Sys. Modell.*, **50**, 6.15-6.16.

Yamaguchi, H., Y. Ichikawa, T. Iwahira, Y. Kuroki, C. Matsukawa, R. Nagasawa, K. Ochi, R. Sekiguchi, T. Takakura, M. Ujiie, and H. Yonehara, 2022: Upgrade of JMA's Global Ensemble Prediction System. *WGNE Res. Activ. Earth Sys. Modell.*, submitted.

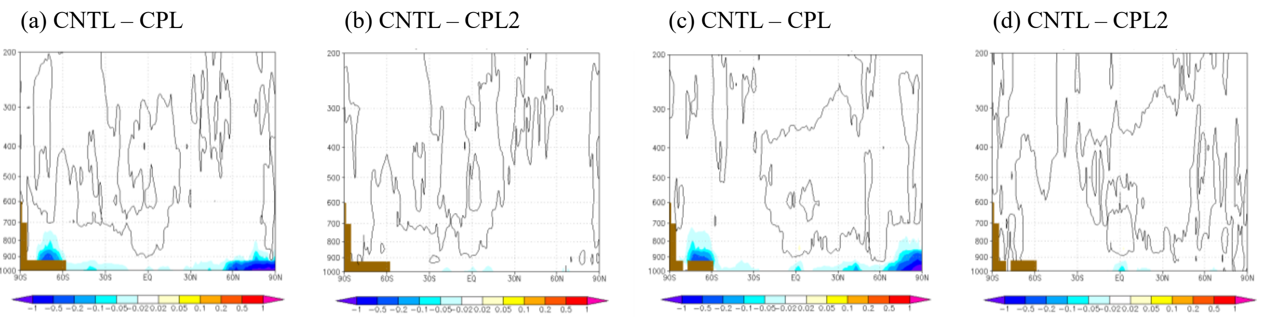

Figure 1 Root mean square error (RMSE) differences against JMA's global analysis in zonal mean temperature (K) at lead times of 24 h in retrospective forecast experiments for (a), (b) winter and (c), (d) summer. Black lines indicate a zero RMSE difference.

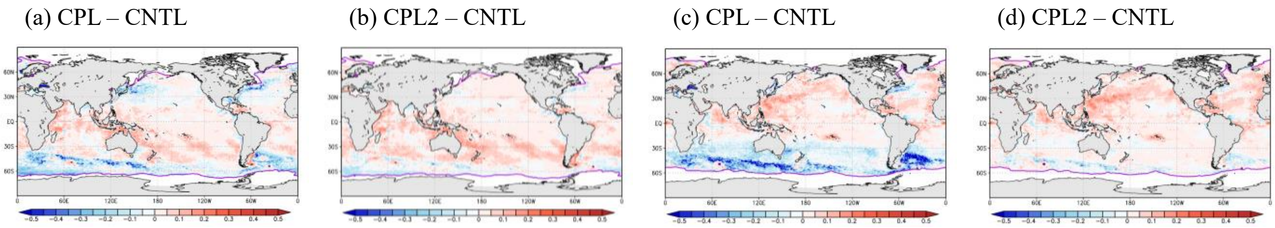

Figure 2 Anomaly correlation coefficient (ACC) differences of ensemble-mean SST over week 1 against ESA SST CCI (Merchant et al. 2014) for (a), (b) winter and (c), (d) summer. The verification period is 1991 – 2015. Areas of sea-ice presence are masked, with purple lines indicating mask boundaries.

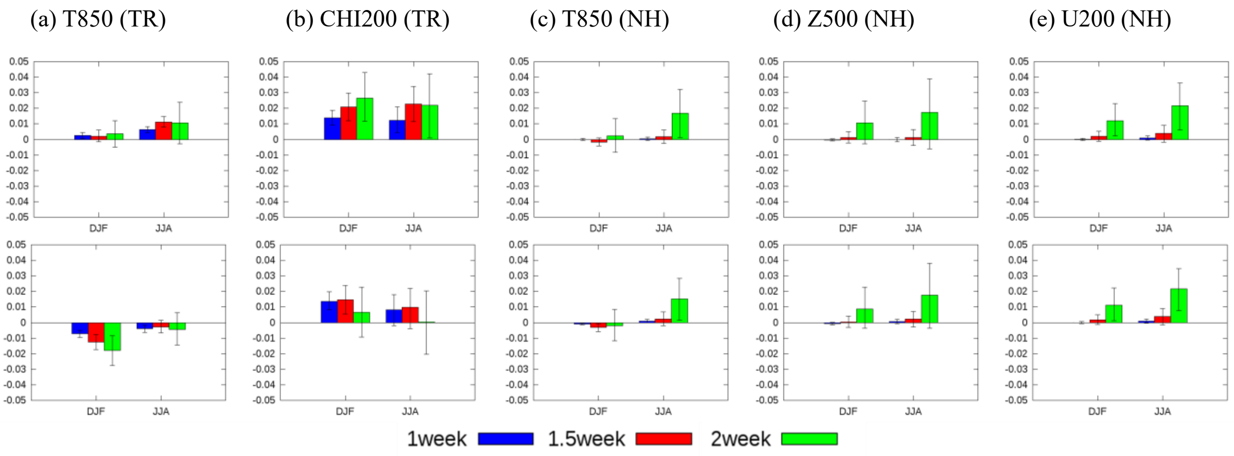

Figure 3 Anomaly correlation coefficient (ACC) differences (top) with bias correction and (bottom) without bias correction for winter (DJF) and summer (JJA). (a) and (b) are in the Tropics (TR; 20°S－20°N), and (c), (d) and (e) are in the Northern Hemisphere (NH; 20－90°N). Each figure shows (a), (c) 850-hPa temperature, (b) 200-hPa velocity potential (d) 500-hPa height and (e) 200-hPa zonal wind. Positive values represent ACCs of CPL2 exceeding those of CNTL. Error bars indicate two-sided 95% confidence levels. ACCs are calculated against JRA-3Q (Kobayashi et al. 2021) for the period from 1991 to 2020.

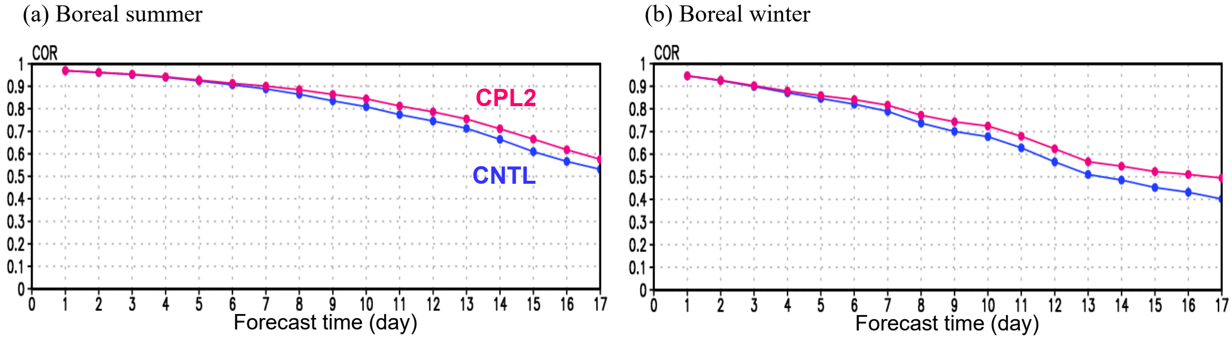

Figure 4 Correlation of MJO index (Matsueda and Endo 2011) in (a) boreal winter and (b) boreal summer. The red and blue lines represent results for CPL2 and CNTL, respectively. The verification period is 1991 – 2020.

Atmospheric River Reconnaissance 2021: Dropsonde Data Impact on GFSv16 Precipitation Forecasts for California

Xingren Wu[1], Keqin Wu[2], Vijay Tallapragada[3], and F.M. Ralph[4]

[1]IMSG at EMC/NCEP/NOAA, College Park, MD 20740
[2]NGI at EMC/NCEP/NOAA, College Park, MD 20740
[3]EMC/NCEP/NOAA, College Park, MD 20740
[4]CW3E, Scripps Institution of Oceanography, UC San Diego, CA 92093

Email: Xingren.Wu@noaa.gov

1. Introduction

Atmospheric rivers (ARs) are long, flowing regions of the atmosphere that carry water vapor through the sky. Water management and flood control in the western United States are heavily influenced by AR storms that produce both beneficial water supply and hazards (Ralph et al. 2020). Due to limited in-situ and ground-based observations (Zheng et al. 2021), aircraft are deployed to collect data in and around the AR systems during AR Reconnaissance (ARR) observational campaigns (Ralph et al. 2020) over the winter of 2016 and 2018-2022. ARR provides additional data by supplementing conventional data assimilation with dropsonde observations of the full atmospheric profile of water vapor, temperature, and winds within ARs. The positive impact of dropsonde data on AR has been reported in several studies (e.g., Lord et al. 2022, Wu et al. 2021, and Zheng et al. 2021).

2. Model and Experiments

In this study the NCEP operational Global Forecast System (GFS) version 16 (GFSv16) was used to examine the impact of the ARR supplemental dropsonde observations on GFS forecasts for a major AR that made landfall along the California coast during January 26-29, 2021. This case study is focused on evaluating a significant weather event that impacted Central California, which experienced AR 2 conditions (based on Ralph et al. 2019 scale) with heavy precipitation. During this ARR observation campaign a series of consecutive flights sampling the same synoptic system from January 23 to 28 were planned and executed.

GFSv16 was implemented into operations in March 2021 at NCEP, with the finite volume cubed-sphere dynamical core and improved GFDL microphysics. Compared to the previous version (GFSv15), GFSv16 increased the number of model vertical layers from 64 to 127, and extended the model top from 55 km to 80 km. The data assimilation (DA) system was upgraded to use a 4-Dimensional Incremental Analysis Update (4D-IAU) technique. The dropsonde data used were from the ARR 2021 campaign during the intensive observation periods (IOPs) from January 17 to March 18, 2021. Global control (Ctrl) and denial (Deny) experiments were conducted by using or denying the dropsonde data in the GFSv16 for both DA and model forecast; the results presented here focus on the forecast from January 24-28 (IOPs 4-8, Cobb 2022).

3. Results

The standard NCEP Metplus verification system was used to evaluate the Ctrl and Deny experiments. Overall the global verification metrics were very similar between Ctrl and Deny, with somewhat better overall forecast skill noted over the Pacific North American (PNA, 180-320E, 20-75N) region when the supplemental dropsonde data were used (not shown). For the case where the prediction skill is relatively low (i.e., the prediction is challenging), the data collected from the dropsondes helped to improve the forecasts and increase the 5-day anomaly correlations, including geopotential height, temperature, and wind. The precipitation prediction over California during January 26-29 improved significantly in Ctrl when the dropsonde data are used (Fig. 1). The improved forecast is associated with improvement in the moisture forecast in Ctrl (not shown), similar to the ARR impact on precipitation forecast for ARR 2020 in GFS version 15 (GFSv15) (Lord et al. 2022).

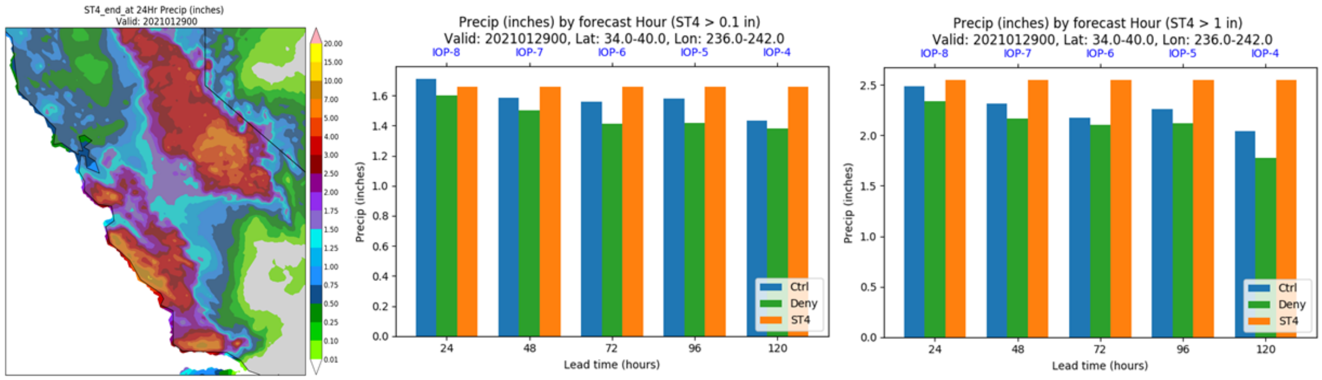

Figure 1 The 24-hour precipitation from January 28 00Z to January 29 00Z over Central and Southern California from Stage IV (left) and the area average precipitation with a cut-off of 0.1 inches (middle) and 1 inches (right) from Stage IV, GFSv16 Ctrl (blue) and Deny (green).

4. Summary

This study indicates that there was a positive impact on the GFS forecast skill for the January 2021 California heavy precipitation event when the dropsonde data were used from consecutive IOPs from the ARR. This is associated with improvement in the moisture and water vapor transport forecasts. The ARR observations helped fill the data gaps needed for DA to provide better model initial conditions (Zheng et al. 2021). There is also a systematic improvement in the precipitation prediction over the U.S. West Coast when the dropsonde data are used, similar to that of ARR 2020 from GFSv15 forecasts (Lord et al. 2022).

Reference:

Cobb, A., and Coauthors, 2022: Atmospheric River Reconnaissance 2021: A Review. Weather and Forecasting, in revision.

Lord, S.J., X. Wu, V. Tallapragada, and F.M. Ralph, 2022: The Impact of Dropsonde Data on the Performance of the NCEP Global Forecast System During the 2020 Atmospheric Rivers Observing Campaign. Part 1: Precipitation. Submitted to Weather and Forecasting.

Ralph, F.M., and Coauthors, 2019: A scale to characterize the strength and impacts of atmospheric rivers. *Bulletin of the American Meteorological Society*, **100**, 269-289, https://doi.org/10.1175/BAMS-D-18-0023.1.

Ralph F.M., and Coauthors, 2020: West Coast forecast challenges and development of Atmospheric River Reconnaissance. *Bulletin of the American Meteorological Society*, **101**, E1357–E1377, https://doi.org/10.1175/BAMS-D-19-0183.1.

Wu, X., V. Tallapragada, S. Lord, K. Wu, and F.M. Ralph, 2021: Impact of Atmospheric River Reconnaissance Dropsonde Data on NCEP GFS Forecast: A Case Study. Research activities in Earth system modelling. Working Group on Numerical Experimentation. Report No. 51. WCRP Report No.4/2021. WMO, Geneva, p. 1-23. http://bluebook.meteoinfo.ru/uploads/2021/sections/BB_21_S1.pdf.

Zheng M., L.D. Monache, X. Wu, F.M. Ralph, B. Cornuelle, V. Tallapragada, J.S. Haase, A.M. Wilson, M. Mazloff, A.C. Subramanian, F. Cannon, 2021: Data Gaps within Atmospheric Rivers over the Northern Pacific. *Bulletin of the American Meteorological Society,* **102**, E492–E524, https://doi.org/10.1175/BAMS-D-19-0287.1. 2021.

Upgrade of JMA’s Global Ensemble Prediction System

YAMAGUCHI Haruki, ADACHI Yukimasa, HIRAHARA Shoji, ICHIKAWA Yuiko, IWAHIRA Tomoya, KUROKI Yukihiro, MATSUKAWA Chihiro, NAGASAWA Ryoji, OCHI Kenta, SEKIGUCHI Ryohei, TAKAKURA Toshinari, UJIIE Masashi, and YONEHARA Hitoshi

Japan Meteorological Agency

e-mail: h.yamaguchi@met.kishou.go.jp

1. Introduction

The Japan Meteorological Agency (JMA) upgraded its Global Ensemble Prediction System (Global EPS) on March 15 2022 to incorporate recent Global Spectral Model (GSM) developments, enhanced horizontal resolution of the model, improved sea surface temperature (SST) boundary conditions and updating of the initial perturbation amplitude.

2. Major Updates

(1) Incorporation of Recent GSM Developments

The forecast model was upgraded to a low-resolution version of the revised Global Spectral Model (GSM), including the following:

- Enhancement of effective resolution, including introduction of a quadratic grid, more subtle coefficients for numerical diffusion operators and more subtle filtering for model orography
- Optimization of parameters for subgrid orographic schemes (Matsukawa et al. 2022)
- Upgrade of diagnostics for effective size of cloud ice for radiation to Sun (2001)
- Improvement for treatment of lake surface temperature, including introduction of climatological data derived from satellite observation
- Upgrade of ozone climatological data based on reanalysis using JMA's latest chemical transport model (MRI-CCM2; Deushi and Shibata 2011) and satellite observation
- Improved calculation of solar zenith angle (Hogan and Hirahara 2016) and treatment of surface albedo (Hogan and Bozzo 2015) for shortwave radiation

(2) Enhanced Horizontal Resolution

As part of plans to improve JMA’s GSM (which provides deterministic medium-range forecasts) Global EPS horizontal resolution was enhanced from around 40 to 27 km for forecasts with lead times up to 432 hours and from 55 to 40 km for 432 to 816 hours. The revised model has a quadratic grid with a triangular truncation wave number of 479 (TQ479) for earlier lead times and 319 (TQ319) for later ones. This supports resolution for coastlines, lakes and small islands, and orography is represented more sharply by the upgraded filtering. Benefits in areas including prediction of winter topographical precipitation in Japan have been noted.

(3) Improved SST Boundary Conditions

SST boundary conditions are given via an approach combining SSTs prescribed as persisting anomalies from climatological values and those operationally precomputed using JMA’s atmosphere-ocean coupled Seasonal EPS model (JMA/MRI-CPS3; Kubo and Ochi 2022). The period for which SSTs in the tropics and subtropics are linearly relaxed from climatological extrapolation to the bias-corrected ensemble mean SST from the Seasonal EPS was also changed from 11 – 18 to 6 – 11 days.

(4) Update of Initial Perturbation Amplitude

The amplitude of singular vector (SV)-based initial perturbations targeted in the 30 – 90°N and 30 – 90°S areas was reduced by 8.7% to mitigate over-dispersiveness in 500 hPa geopotential height forecasts with lead times of up to four days.

3. Verification Results

To verify system performance for medium-range forecasts with lead times of up to 11 days, retrospective forecast experiments covering periods of three months or more in winter 2019/20 and summer 2020 were conducted. The results showed improvements of ensemble mean forecasts for several elements, including 850 hPa temperature, 500 hPa geopotential height and 250 hPa winds globally for both seasons. Figure 1 shows RMSEs of ensemble mean forecasts for 500 hPa geopotential height and 850 hPa temperature for the Northern Hemisphere in winter. Brier skill scores for precipitation forecasts in Japan were also improved (not shown). Performance for forecasts beyond 11 days was also verified, as reported by Sekiguchi et al. (2022).

References

Deushi, M., and K. Shibata, 2011: Development of a Meteorological Research Institute Chemistry-Climate Model version 2 for the Study of Tropospheric and Stratospheric Chemistry. *Pap. Meteorol. Geophys.*, 62, 1-46.

Hogan, R.J. and Bozzo, A., 2015. Mitigating errors in surface temperature forecasts using approximate radiation updates. *J. Adv. Model. Earth Syst.*, 7, 836-853.

Hogan, R.J. and Hirahara, S., 2016. Effect of solar zenith angle specification in models on mean shortwave fluxes and stratospheric temperatures. *Geophys. Res. Lett.*, 43, 482-488.

Kubo Y., and K. Ochi, 2022: Verification of JMA/MRI-CPS3 and JMA Global Ensemble Prediction System in the sub-seasonal forecast. *WGNE Res. Activ. Earth Sys. Modell.*, submitted.

Matsukawa C., Y. Kuroki, and T. Kanehama, 2022: Optimization of orographic drag parametrizations in the JMA operational global model using COORDE-type experiments. *WGNE Res. Activ. Earth Sys. Modell.*, submitted.

Sekiguchi, R., Y. Ichikawa, K. Ochi, and T. Takakura, 2022: Hindcast verification of JMA's GEPS for one-month prediction. *WGNE Res. Activ. Earth Sys. Modell.*, submitted.

Sun, Z., 2001: Reply to comments by Greg M. McFarquhar on ‘Parametrization of effective sizes of cirrus-cloud particles and its verification against observations’. (October B, 1999, 125, 3037–3055). *Q. J. R. Meteorol. Soc.*, 127, 267-271.

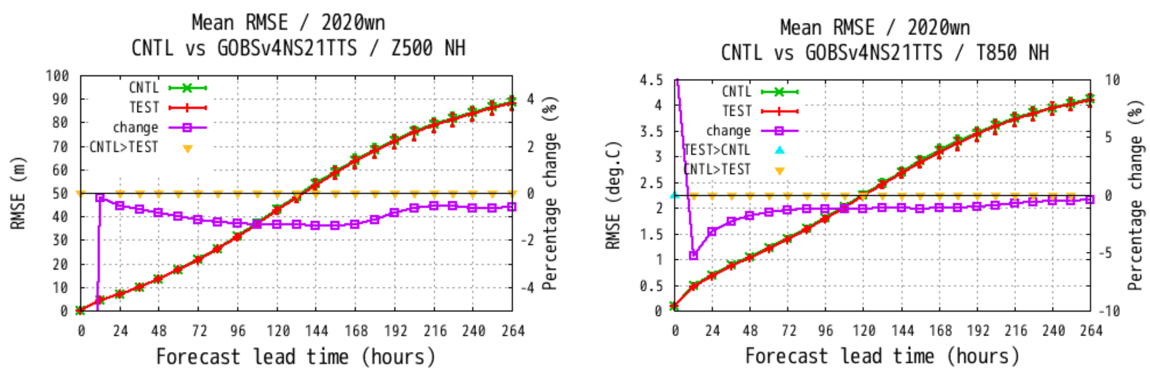

Figure 1: RMSEs of 500 hPa geopotential height [m] and 850 hPa temperature [°C] ensemble mean forecasts against analysis for the Northern Hemisphere (20 – 90°N) during winter 2019/20 as a function of forecast lead times up to 264 hours. The red and green lines represent verification results for the new (TEST) and previous (CNTL) Global EPS (left axis; unit: m), and the purple line represents ratios of change in scores ([TEST – CNTL]/CNTL, right axis; unit: %). Error bars indicate two-sided 95% confidence levels, and triangles (TEST < CNTL or CNTL > TEST) indicate a statistically significant difference of 0.05.

Assimilation of 2-m temperatures and adaptive adjustment of uncertain model parameters building upon it

Günther Zängl and Harald Anlauf
Deutscher Wetterdienst, Offenbach, Germany
E-mail: Guenther.Zaengl@dwd.de

1 Introduction

In NWP models, near-surface forecast variables like 2-m temperature (T2M) or 2-m relative humidity (RH2M) can be subject to substantial systematic forecast errors for a variety of reasons, e.g. limited quality of external parameter data and physical properties of soil and vegetation derived therefrom, poor knowledge of soil moisture in deeper layers, and simplifications or inadequacies in the parameterization of related physical processes. Attributing specific biases to one of these potential sources is difficult due to the lack of data, and tuning exercises frequently end up with improvements in some regions or seasons and degradations in others. In particular, transient model biases cannot be reduced this way. Moreover, the assimilation of 2-m variables suffers from the presence of substantial model errors. Assimilating T2M even tends to degrade the lower-tropospheric analysis quality if the data assimilation has to act against severe model biases, and therefore, only RH2M has been assimilated in DWD's operational global ICON forecasting system (Zängl et al., 2015) so far. Significant progress could be made, however, by a co-development between model and data assimilation, using information from data assimilation to adaptively adjust uncertain model parameters in order to minimize systematic errors.

2 Methodology

Our algorithm builds upon the assimilation of RH2M and T2M by computing time-filtered assimilation increments of temperature and humidity at the lowest model level, which are subsequently used as a proxy for the respective model biases. Time-filtering is accomplished by a Newtonian relaxation approach with a time scale of 2.5 days, which is needed to separate random from systematic errors and to remove possible diurnal cycles from the average biases. In addition, a filtered temperature increment weighted by the cosine of local time is calculated as a proxy for the diurnal temperature amplitude bias.

Based upon these quantities, a variety of model parameters whose basic values are either tuning parameters or estimated from external parameter data are adaptively adjusted in order to minimize systematic model errors. Specifically, average temperature and humidity increments are used over snow-free land surfaces to vary the minimum stomata resistance of plants and a tuning parameter for scaling bare-soil evaporation. They are used to define a combined temperature-humidity bias $TRH_b = \alpha RH_{if} - \beta T_{if}$, where RH_{if} and T_{if} are the time-filtered assimilation increments and α and β are positive tuning parameters (noting that assimilation increments have the opposite sign as the model bias). Based upon this, a model parameter ψ having a reference value ψ_r is modified according to

$$\psi = \psi_r/(1 + TRH_b) \text{ if } TRH_b > 0 \quad ; \quad \psi = \psi_r\,(1 - TRH_b) \text{ if } TRH_b < 0 \tag{1}$$

if ψ needs to be reduced in order to mitigate a warm bias; otherwise multiplication and division are reversed. On snow-covered land surfaces, a similarly defined pure temperature bias is used to vary the snow albedo otherwise depending on vegetation cover and snow aging. Moreover, to reduce biases in the diurnal temperature amplitude, the above-mentioned weighted increment is used to vary the heat conductivities of the soil and the skin layer as well as the soil heat capacity using a similar algorithmic approach.

3 Results

The changes presented here have been operationalized in the global ICON forecasting system of DWD in May 2022. Extensive experiments conducted in the preparatory phase indicated that the direct impact of the T2M assimilation is rather short-lived, typically decaying to zero after two forecast days. However, exploiting the potential for adaptive model parameter adjustment substantially prolongates the beneficial impact not only for T2M, but also for RH2M. This is illustrated in Fig. 1, showing the relative RMSE improvements for the extratropical hemispheres and the tropics for a 2.5-month period in late 2020. In all regions, statistically significant improvements are obtained for both variables during the whole forecast range (180 h).

A closer analysis reveals that the improvements exhibit strong regional (and also seasonal) variability because they are proportional to the magnitude of the model biases in the reference configuration. Particularly large benefits have been obtained in several central Asian regions, where the diurnal temperature amplitude used to be significantly underestimated, and in snow-covered regions, where the uncertainties of the albedo and heat conductivity generally enhance the forecast errors. Reducing model errors of the diurnal temperature amplitude was in turn found to be important for the quality of the analyses. Specifically, a nocturnal warm model bias tends to induce cooling increments extending over a too deep layer, degrading the analysis quality between about 500 m and 1000 m above ground (as indicated by the radiosonde verification; not shown). Thus, the initially mentioned co-development between model and data assimilation was indeed crucial for the successful implementation of this ugrade.

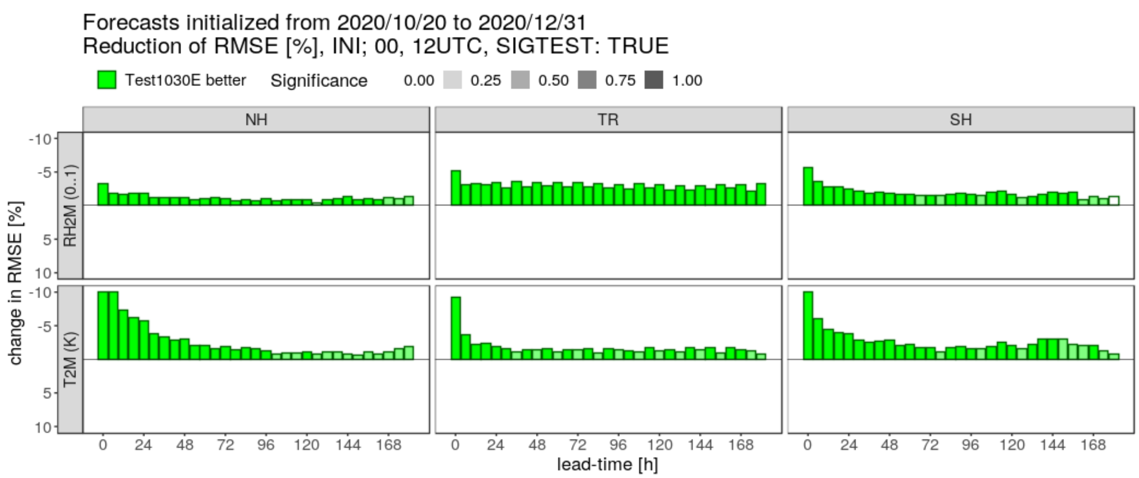

Figure 1: Relative RMSE improvements achieved due to the T2M assimilation and the related model parameter coupling for an experiment period in autumn/winter 2020. Color filling indicates significance at the 95% level.

Reference

Zängl, G., D. Reinert, P. Ripodas and M. Baldauf, 2015: The ICON (ICOsahedral Nonhydrostatic) modelling framework of DWD and MPI-M: Description of the nonhydrostatic dynamical core. *Quart. J. Roy. Met. Soc.,* **141**, 563–579.